

Decomposition of unitary matrices for finding quantum circuits: Application to molecular Hamiltonians

Anmer Daskin¹ and Sabre Kais^{2,a)}

¹Department of Computer Science, Purdue University, West Lafayette, Indiana 47907, USA

²Department of Chemistry, Physics, and Birck Nanotechnology Center, Purdue University, West Lafayette, Indiana 47907, USA

(Received 10 January 2011; accepted 21 March 2011; published online 14 April 2011)

Constructing appropriate unitary matrix operators for new quantum algorithms and finding the minimum cost gate sequences for the implementation of these unitary operators is of fundamental importance in the field of quantum information and quantum computation. Evolution of quantum circuits faces two major challenges: complex and huge search space and the high costs of simulating quantum circuits on classical computers. Here, we use the group leaders optimization algorithm to decompose a given unitary matrix into a proper-minimum cost quantum gate sequence. We test the method on the known decompositions of Toffoli gate, the amplification step of the Grover search algorithm, the quantum Fourier transform, and the sender part of the quantum teleportation. Using this procedure, we present the circuit designs for the simulation of the unitary propagators of the Hamiltonians for the hydrogen and the water molecules. The approach is general and can be applied to generate the sequence of quantum gates for larger molecular systems. © 2011 American Institute of Physics. [doi:10.1063/1.3575402]

I. INTRODUCTION

Quantum computation promises to solve fundamental, yet otherwise intractable, problems in many different fields. To advance the quantum computing field, finding circuit designs to execute algorithms on quantum computers (in the circuit model of quantum computing) is important. Therefore, it is of fundamental importance to develop new methods with which to overcome the difficulty in forming a unitary matrix describing the algorithm (or the part of the computation), and the difficulty to decompose this matrix into the known quantum gates.¹ Realizing the theoretical problems of quantum computers requires the overcoming decoherence problem.² Recently, West *et al.* demonstrated numerically that high fidelity quantum gates are possible in the frame work of quantum dynamic and decoupling.³

It has been shown that the ground and excited state energies of small molecules can be carried out on a quantum computer simulator using a recursive phase-estimation algorithm.⁴⁻⁷ Lanyon *et al.* reported the application of photonic quantum computer technology to calculate properties of the hydrogen molecule in a minimal basis.⁸ For the simulation of quantum systems, it is needed to find efficient quantum circuits.

The problem in the decomposition of a given unitary matrix into a sequence of quantum logic gates can be presented as an optimization problem. Williams and Gray⁹ suggested the use of genetic programming technique to find new circuit designs for known algorithms and also presented results for the quantum teleportation. Yabuki, Iba,¹⁰ and Peng *et al.*¹¹ focused on circuit designs for the quantum teleportation by

using different genetic algorithm techniques. Spector¹² explains the use of genetic programming to explore new quantum algorithms. Stadelhofer¹³ used the genetic algorithms to evolve black box quantum algorithms. There are also some other works¹⁴⁻¹⁶ which evolve quantum algorithms or circuits by using the genetic programming or the genetic algorithms. Review of these procedures can be found in Ref. 17. The evolution of quantum circuits faces two major challenges: complex and huge search space and the high costs of simulating quantum circuits on classical computers. In this paper, we use our recently developed group leaders optimization algorithm (GLOA)¹⁸—an evolutionary algorithm—to decompose the unitary matrices into a set of quantum gates. We show how our approach can be used to find the circuit representation of a quantum algorithm or the unitary propagator of a quantum system, which is essential to perform the simulation. The approach was tested on the operators of the Grover search algorithm; the sender part of the quantum teleportation; the Toffoli gate; and the quantum Fourier transform. It was also used to find the circuit designs for the simulations of the hydrogen and the water molecules on quantum computers.

This paper is organized as follows: after giving the essentials of the objective function in Sec. II, we give the optimization results for quantum algorithms in Sec. III. And in Sec. IV we explain how the method can be used to design circuits for the simulation of molecular Hamiltonians and present the circuit designs and their simulations within the phase estimation algorithm for the hydrogen and water molecules.

II. THE OVERVIEW OF THE OPTIMIZATION SCHEME

A. The objective

The objective of the optimization process is to find quantum circuits with minimum costs and errors. Thus, there

^{a)}Author to whom correspondence should be addressed. Electronic mail: kais@purdue.edu.

are two factors which need to be optimized within the optimization: the error and the cost of the circuit. The minimization of the error to an acceptable level is more important than the cost in order to get more accurate and reliable results in the optimization process (The importance of the cost and the error in the approximated circuit can be adjusted by an objective function constituting both with some weights); hence, in the optimization the circuit giving a better approximation to the solution is always preferred over the other circuit with a lower cost.

1. The fidelity error

For the unitary matrix representation of a candidate approximation circuit, U_a , in the optimization and a given target unitary matrix U_t , Williams and Gray⁹ described the quality of the circuit as follows:

$$f(U_a, U_t) = \sum_{i=1}^{2^n} \sum_{j=1}^{2^n} |U_{t(ij)} - U_{a(ij)}|, \quad (1)$$

where U_t and $U_a \in U^{2^n}$ and $f = 0$ when $U_t = U_a$. Since the global phase differences between two quantum systems are physically indistinguishable; when U_t and U_a are different only in terms of their global phases, the value of f should be zero. However, Eq. (1) is unlikely to produce zero for this case. Here, instead of Eq. (1), we use the trace fidelity error which ignores the global phase differences; hence, makes the optimization easier by diversifying the reachable solutions for a problem in complex space. The trace fidelity is given by

$$\mathcal{F} = \frac{1}{N} \left| \text{Tr} \left(U_a U_t^\dagger \right) \right|, \quad (2)$$

where $N = 2^n$ (n is the number of qubits); the symbol \dagger represents the complex conjugate transpose of a matrix; and $\text{Tr}(\dots)$ is the trace of a matrix. Since the product of two unitary matrices is another unitary matrix all eigenvalues of which have absolute value 1, \mathcal{F} is always in the range $[0, 1]$ and is equal to 1 when $U_a = U_t$. The fidelity error used in the optimization to measure how similar the unitary operators U_a and U_t are is defined as¹⁹

$$\epsilon = 1 - \mathcal{F}^2, \quad (3)$$

where \mathcal{F} is squared to increase the effects of small fidelity changes in the error.

2. The cost of a circuit

The cost of a circuit describes the level of ease with which this circuit is implemented; in order to make the implementation of a circuit easier and the circuit less error-prone, the cost also needs to be optimized by minimizing the number of gates in the circuit.

However, defining the cost of a circuit is not an easy task due to the fact that each quantum computer model may have a different cost for a given quantum gate. Here, the costs of a one-qubit gate and a control (two-qubit) gate are defined as 1 and 2, respectively. Since the implementation of a multi-

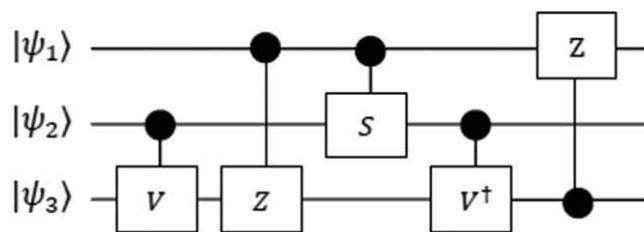


FIG. 1. The circuit design for the Toffoli gate.

control gate (n -qubit network) requires $\Theta(2^n)$ (see Ref. 20), its cost is defined as 2^n where n is the number of qubits on which the gate is operating. The cost of a circuit is found by summing up the costs of the gates composing the circuit. For instance, the cost of the circuit in Fig. 1 is 10. The real implementation cost of a circuit may be different than this abstraction; nevertheless, a lower-cost circuit found in the optimization likely costs less than a higher-cost circuit in the implementation.

B. The representation of quantum gates in the optimization

We use similar representation method to the method of the Cartesian genetic programming²¹ in which each function set and inputs (in our case, gates and qubits) are represented as integers and genotypes including the inputs and the gates, which are represented as integer strings. The difference is since the quantum gates may have an effect on the whole system, the gates should be represented in time steps; that means we cannot give the same inputs to two different gates at the same time as it is done in classical circuits. In the strings of the genotypes each four numbers represent a gate, the qubit on which the gate operates, the control qubit, and the angle for the rotation gates. The integers for gates are determined by looking at the indices of the gates in the gate set. For a given set of gates $\{V, Z, S, V^\dagger\}$ (see Appendix for the matrix representation of these gates), an example of numeric string representing the circuit in Fig. 1 is as

$$\mathbf{1} \ 3 \ 2 \ 0.0; \mathbf{2} \ 3 \ 1 \ 0.0; \mathbf{3} \ 2 \ 1 \ 0.0; \mathbf{4} \ 3 \ 2 \ 0.0; \mathbf{2} \ 1 \ 3 \ 0.0,$$

where the each group of four numbers separated by semicolons describes the each quantum gate in the circuit: the first numbers with bold fonts identify the gates ($\{V = 1, Z = 2, S = 3, V^\dagger = 4\}$), the last numbers are the values of the angles between 0 and 2π (for nonrotation gates it is considered 0.), and the middle integers are the target and the control qubits, respectively, (the semicolons and the bold fonts do not appear in the real implementation). For multicontrol gates the qubits between the control and the target qubits are also considered as control qubits.

The length of a numeric string is the maximum number of gates a circuit can include. The required maximum number of gates can be very large: Suppose U acts on a 2^n -dimensional Hilbert subspace. Then U may be written as a product of at most $2^{n-1}(2^n - 1)$ two-level unitary systems.¹ For five-qubits, there may be 496 two-level unitary matrices required to form

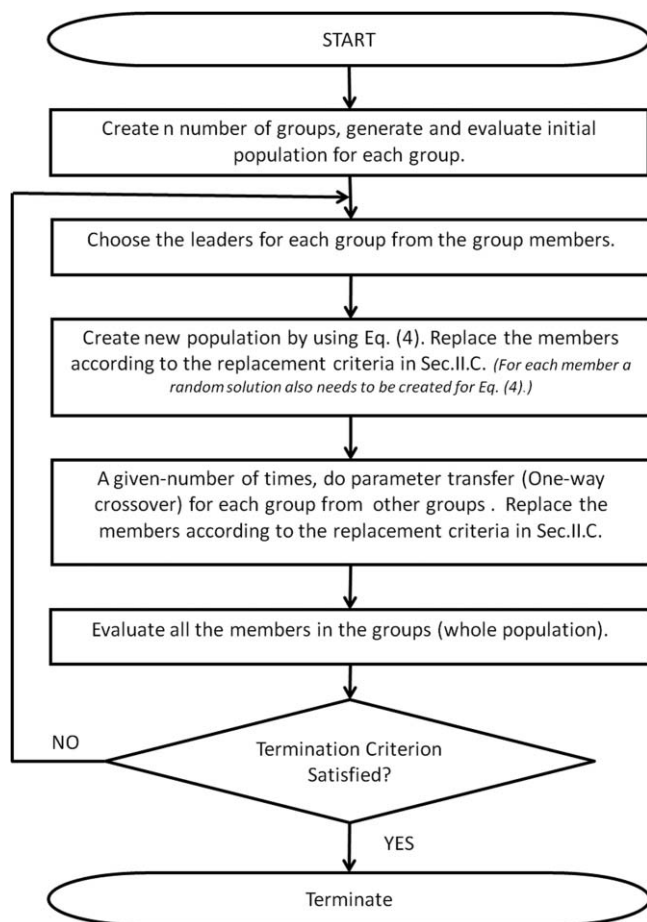


FIG. 2. The flow chart of the group leaders optimization algorithm.

a given U . In our optimization cases, the maximum number of gates (\max_{gates}) is limited to 20 gates.

C. The group leaders optimization algorithm

The group leaders optimization algorithm described in more detail in Ref. 18 is a simple and effective global optimization algorithm that models the influence of leaders in social groups as an optimization tool. The general structure of the algorithm is made up by dividing the population into several disjunct groups each of which has its leader (the best member of the group) and members. The algorithm which is different from the earlier evolutionary algorithms and the pivot method algorithm^{22–24} consists of two parts. In the first part, the member itself the group leader with possible random part and a new-created random solution are used to form a new member. This mutation is defined as

$$\begin{aligned} \text{new member} = & r_1 \text{ portion of old member} \\ & \cup r_2 \text{ portion of leader} \\ & \cup r_3 \text{ portion of random,} \end{aligned} \quad (4)$$

where r_1 , r_2 , and r_3 determine the rates of the old member, the group leader, and the new-created random solution into the new formed member and they sum to 1. In our case,

they are set as $r_1 = 0.8$ and $r_2 = r_3 = 0.1$. The mutation for the values of the all angles in a numerical string is done according to the arithmetic expression: $\text{angle}_{\text{new}} = r_1 \times \text{angle}_{\text{old}} + r_2 \times \text{angle}_{\text{leader}} + r_3 \times \text{angle}_{\text{random}}$, where $\text{angle}_{\text{old}}$, the current value of an angle, is mutated; $\text{angle}_{\text{new}}$, the new value of the angle, is formed by combining a random value and the corresponding leader of the group of the angle and the current value of the angle with the coefficients r_1 , r_2 , and r_3 . The mutation for the rest of the elements in the string means the replacement of its elements by the corresponding elements of the leader and a newly generated random string with the rates r_2 and r_3 .

In addition to the mutation, in each iteration for each group of the population one-way-crossover (also called the parameter transfer) is done between a chosen random member from the group and a random member from a different random group. This operation is mainly replacing some random part of a member with the equivalent part of a random member from a different group. The amount of the transfer operation for each group is defined by a parameter called transfer rate, here, which is defined as $\frac{4 \times \max_{\text{gates}}}{2} - 1$, where the numerator is the number of variables forming a numeric string in the optimization.

1. The replacement criteria

If a new formed (or mutated) member gives less error-prone solution to the problem than the corresponding old member, or they have the same error values but the cost of the new member is less than the old member, then the new member survives and replaces the old member; otherwise, the old member remains for the next iteration and the new one formed is discarded.

The flow chart of the algorithm for our optimization problem is drawn in Fig. 2. For more information about the algorithm, the reader is referred to Ref. 18.

D. Parameters in the optimization

The parameters for the algorithm and \max_{gates} are defined in subsections II B and II C, the rest of the parameters used in the optimization are defined as follows: The default gate set consists of the rotation gates (R_x , R_y , R_z , R_{zz}); X , Y , Z which are the Pauli operators σ_x , σ_y , and σ_z , respectively; the square root of X gate (V); the complex conjugate of V gate (V^\dagger), S gate, T gate, and H (Hadamard) gate; and the controlled versions of these gates. For the matrix representation of these gates, please see Appendix. The angle values for the rotation gates are taken as in the range $[0, 2\pi]$.

The test cases are divided into two categories: the known quantum algorithms and the unitary propagators of the molecular Hamiltonians. In the case of quantum algorithms the number of iterations is limited to 6000 iterations for the four-qubit quantum Fourier transform and 2000 for the rest while in the case of molecular Hamiltonians it is limited to 15 000. For both cases, the parameters of the algorithm: the number of group is set to 25 and the number of population in each group is set to 15; so the total initial population is 375. Sections III and IV give and discuss the results.

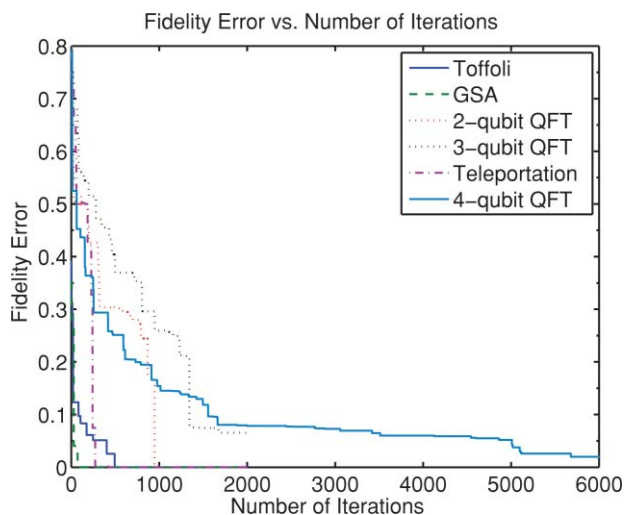


FIG. 3. The evolution of the fidelity error for quantum algorithms.

III. CIRCUIT DESIGNS FOR THE QUANTUM ALGORITHMS

The circuit designs for the cases of the known algorithms are not only important to find different circuit designs which may ease the implementation difficulties in different quantum computer models but also to test the correctness, the efficiency, and the reliability of the optimization method on known results before using it to find the circuit representations of the more complex cases and the cases where the characteristics of the solutions are unknown. Hence, we use the optimization method to measure the ability of the method by finding circuit designs for the Toffoli gate, the Grover search algorithm, the quantum Fourier transform, and the quantum teleportation. The more details about these algorithms can be found in Ref. 1. The resulting circuit designs with the descriptions of the problems are given in subsections III A–III D. For each case, the evolution of the minimum fidelity error with respect to the number of iterations is plotted in Fig. 3.

A. The Toffoli gate

The Toffoli gate has two controls, the first and the second, qubits and one target, the third, qubit (see Appendix for the matrix representation). The circuit diagram for the unitary matrix of this gate shown in Fig. 1 which has the same length as the known circuit designs (see Ref. 25). The algorithm reaches the exact solution in 500 iterations as shown in Fig. 3.

B. The amplification part of the Grover search algorithm

Grover's algorithm searches an unstructured N -element list in $O(\sqrt{N})$ time compared to its classical counterpart which is $O(N)$. The unitary operator for the amplification part of the Grover search algorithm (GSA) is constructed as²⁶

$$D_{ij} = \begin{cases} \frac{2}{N}, & \text{if } i \neq j \\ -1 + \frac{2}{N}, & \text{if } i = j \end{cases}. \quad (5)$$

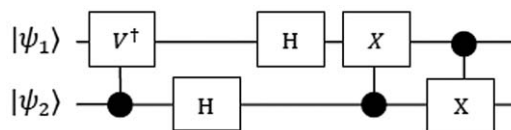


FIG. 4. The circuit design for the two-qubit quantum Fourier transform.

The algorithm reaches the explicit circuit diagram for the operator D for two-qubits shown in Fig. 5 after 100 iterations, which is shown in Fig. 3.

C. The quantum Fourier transform

The quantum Fourier transform (QFT) is one of the key ingredients of the quantum factoring algorithm and many other quantum algorithms. The unitary operator of the QFT is constructed as¹

$$\frac{1}{\sqrt{2^n}} \begin{pmatrix} 1 & 1 & 1 & \cdots & 1 \\ 1 & w & w^2 & \cdots & 1 \\ 1 & w^2 & w^4 & \cdots & w^\beta \\ 1 & w^3 & w^6 & \cdots & w^{2\beta} \\ \vdots & \vdots & \vdots & \ddots & \vdots \\ 1 & w^\beta & w^{2\beta} & \cdots & w^{\beta^2} \end{pmatrix}, \quad (6)$$

where $\beta = 2^n - 1$ and $w = e^{2\pi i/2^n}$.

In our optimization, we use the two-, three-, and four-qubit quantum Fourier transforms for which the circuit designs are found as in Figs. 4, 6, and 7, respectively. The approximated circuit for the three-qubit case consists of eight gates: five control and three single gates, while the circuit design for the same case in Ref. 1 consists of six control gates and requires swap operations at the end of the circuit. In Fig. 7, 13 control and four single gates form the approximated circuit for the four-qubit QFT in which there is only one more control gate in comparison to the general circuit design of the QFT given in Ref. 1 (the swap gates are also included in the comparison). While the result for the two-qubit case is exact, for the three- and the four-qubit cases small fidelity errors exist as shown in Fig. 3 because of the approximation of the angle values for the two rotation gates in the circuit.

D. The quantum teleportation

Suppose Alice who has the first qubit wants to send information to Bob who has the second qubit. Quantum teleportation is a protocol which allows Alice to communicate an unknown quantum state of a qubit by using two classical bits in a way that Bob is able to reproduce the exact original state from these two classical bits.^{1,27} Here, only the sender part of

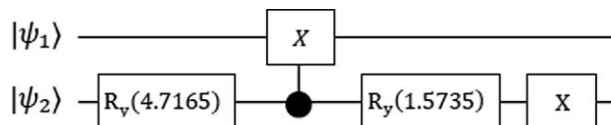


FIG. 5. The circuit design for the two-qubit amplification part of the Grover search algorithm.

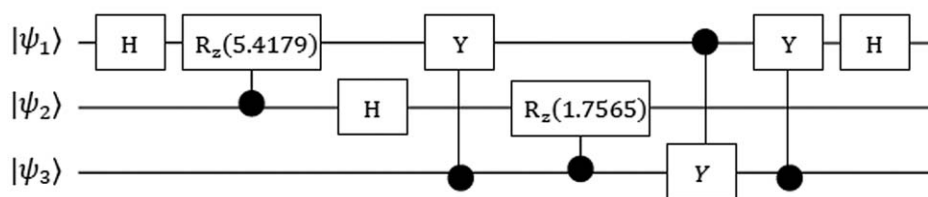


FIG. 6. The circuit design for the three-qubit quantum Fourier transform.

the quantum teleportation is used in the optimization since the unitary operator of the receiver part of the algorithm is similar to the sender part. The matrix representation of the sender part of the algorithm is given in Appendix. Figure 8 shows the resulting circuit design for this matrix which is found in 300 iterations (see Fig. 3). The circuit design in Fig. 8 consists of four gates and has the same length as that of the most well known and efficient circuit designs given in Refs. 9 and 28.

IV. CIRCUIT DESIGNS FOR THE SIMULATION OF MOLECULAR HAMILTONIANS

Finding the low cost circuit representations of complex exponentials of the molecular Hamiltonians are important to be able to perform simulations on quantum computers. Here, after explaining the electronic Hamiltonian in the second quantized form and how to map the fermionic quantum operators to the standard quantum operators, we show how to use the optimization method to find quantum circuits for the molecular Hamiltonians and the simulation results for the water and the hydrogen molecules within the phase estimation algorithm.

Fermion model of quantum computation is defined through the spinless fermionic annihilation (a_j) and creation (a_j^\dagger) operators for each qubit j ($j = 1, \dots, n$), where the algebra of $2n$ elements obey the fermionic anticommutation rules:²⁹

$$\{a_i, a_j\} = 0, \{a_i, a_j^\dagger\} = \delta_{ij}, \quad (7)$$

where $\{A, B\} = AB + BA$ defines the anticommutator. Using the Jordan–Wigner transformation,³⁰ the fermion operators are mapped to the standard quantum computation operators through the Pauli spin operators:

$$a_j \rightarrow \left(\prod_{k=1}^{j-1} -\sigma_z^k \right) \sigma_-^j = (-1)^{j-1} \sigma_z^1 \sigma_z^2 \dots \sigma_z^{j-1} \sigma_-^j$$

$$a_j^\dagger \rightarrow \left(\prod_{k=1}^{j-1} -\sigma_z^k \right) \sigma_+^j = (-1)^{j-1} \sigma_z^1 \sigma_z^2 \dots \sigma_z^{j-1} \sigma_+^j. \quad (8)$$

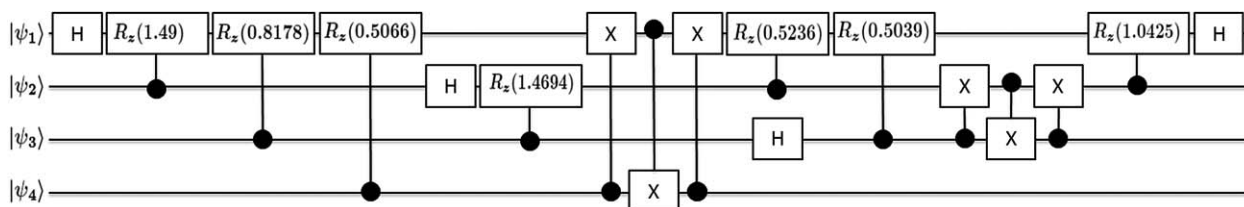


FIG. 7. The circuit design for the four-qubit quantum Fourier transform.

Once the electronic Hamiltonian is defined in second quantized form, the state space can be mapped to qubits. The molecular electronic Hamiltonian, in the Born–Oppenheimer approximation, is described in the second quantization form as^{8,31,32}

$$\mathcal{H} = \sum_{pq} h_{pq} a_p^\dagger a_q + \frac{1}{2} \sum_{pqrs} h_{pqrs} a_p^\dagger a_q^\dagger a_s a_r, \quad (9)$$

where the matrix elements h_{pq} and h_{pqrs} are the set of one- and two-electron integrals. Let the set of single-particle spatial functions constitute the molecular orbitals $\{\varphi(\mathbf{r})\}_{k=1}^M$ and the set of spin orbitals $\{\chi(\mathbf{x})\}_{p=1}^{2M}$ be defined with $\chi_p = \varphi_i \sigma_i$ and the set of space-spin coordinates $\mathbf{x} = (\mathbf{r}, \omega)$ where σ_i is a spin function. The one-electron integral is defined as³¹

$$h_{pq} = \int d\mathbf{x} \chi_p^*(\mathbf{x}) \left(-\frac{1}{2} \nabla^2 - \sum_{\alpha} \frac{Z_{\alpha}}{r_{\alpha\mathbf{x}}} \right) \chi_q(\mathbf{x})$$

$$= \langle \varphi_p | H^{(1)} | \varphi_q \rangle \delta_{\sigma_p \sigma_q} \quad (10)$$

and the two electron integral is

$$h_{pqrs} = \int d\mathbf{x}_1 d\mathbf{x}_2 \frac{\chi_p^*(\mathbf{x}_1) \chi_q^*(\mathbf{x}_2) \chi_s(\mathbf{x}_1) \chi_r(\mathbf{x}_2)}{r_{12}}$$

$$= \langle \varphi_p | \langle \varphi_q | H^{(2)} | \varphi_r \rangle | \varphi_s \rangle \delta_{\sigma_p \sigma_q} \delta_{\sigma_r \sigma_s}, \quad (11)$$

where $r_{\alpha\mathbf{x}}$ is the distance between the α th nucleus and the electron, r_{12} is the distance between electrons, ∇^2 is the Laplacian of the electron spatial coordinates, and $\chi_p(\mathbf{x})$ is a selected single-particle basis: $\chi_p = \varphi_p \sigma_p$, $\chi_q = \varphi_q \sigma_q$, $\chi_r = \varphi_r \sigma_r$, and $\chi_s = \varphi_s \sigma_s$. For detailed description of quantum computation for molecular energy simulations, see Whitfield *et al.*³¹

A. Phase estimation algorithm

Quantum computing provides an efficient method, the phase estimation algorithm (PEA),^{4,33,34} to estimate the energy eigenvalues of a molecular Hamiltonian.³⁵ Suppose we have the unitary operator $U = e^{-i\mathcal{H}t/\hbar}$ for a Hamiltonian \mathcal{H}

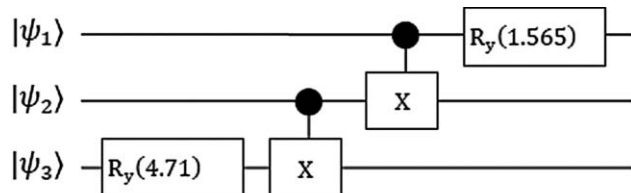


FIG. 8. The circuit design for the sender part of the quantum teleportation.

with energy eigenstates $|\psi_j\rangle$ corresponding energy eigenvalues E_j , i.e., $\mathcal{H}|\psi_j\rangle = E_j|\psi_j\rangle$. Since E_j is an eigenvalue of \mathcal{H} ; if t and \hbar are set to 1, then $e^{-iE_j t}$ is the eigenvalue of the unitary operator U . Therefore, $N \times N$ unitary transformation U has an orthonormal basis of eigenvectors $|\varphi_1\rangle, |\varphi_2\rangle, \dots, |\varphi_N\rangle$ with eigenvalues $\lambda_j = e^{2\pi i \phi_j}$. The iterative PEA depicted in Fig. 9 can be used to estimate the value of the phase ϕ_j which also allows us to determine the corresponding eigenvalue E_j of the Hamiltonian \mathcal{H} . The phase ϕ_j is obtained from the measurement results described as a binary expansion:

$$\begin{aligned} \phi_j &= (0.\phi_1\phi_2 \dots \phi_m)_{\text{binary}} \\ &= \phi_1 2^{-1} + \phi_2 2^{-2} \dots \phi_{m-1} 2^{-m+1} + \phi_m 2^{-m}. \end{aligned} \quad (12)$$

To find the circuit equivalence of U^{2^k} in Fig. 9 the angle values of the rotation gates in the circuit represented by U are multiplied by 2^k in each k th iteration of the algorithm since $R_x(\theta)^{2^k} = R_x(2^k\theta)$, $R_y(\theta)^{2^k} = R_y(2^k\theta)$, and $R_z(\theta)^{2^k} = R_z(2^k\theta)$.

B. Simulation of the hydrogen molecule

The key challenge of exact quantum chemistry calculations is the exponential growth of our description of the wave function with the number of atoms. Consider a simple molecule such as methanol. Using only the 6-31G** basis for the valence electrons, there are 50 orbitals. The 18 valence electrons can be distributed in these orbitals in any way that satisfies the Pauli exclusion principle. This leads to about 10^{17} possible configurations making an exact or full configuration interaction (FCI) calculation impossible. Recently, a quantum algorithm for the solution of the FCI problem in polynomial time was proposed by Aspuru-Guzik *et al.*⁵ This algorithm employed the Hartree–Fock wave function as a reference for further treatment of the correlation effects by the FCI Hamiltonian on the quantum computer. Using an optical quantum computer, Lanyon *et al.*⁸ presented an experimental realiza-

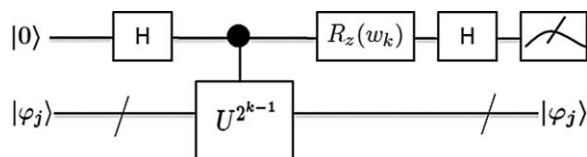


FIG. 9. The iterative phase estimation algorithm for the k th iteration.^{4,33,34} In the circuit $|\varphi_j\rangle$ is an eigenvalue of U , and the angle w_k of the R_z gate depends on the previous measured bits defined as $w_k = -2\pi(0.0\phi_k\phi_{k-1}\dots\phi_m)_{\text{binary}}$, where m is the number of digits determining the accuracy of the phase ϕ_j . Note that w_k is zero at the first iteration of the algorithm.

tion of quantum simulation of the energy spectrum of the hydrogen molecule. The key limitation in it is the representation of the simulated system's propagator.

One spatial function is needed per atom denoted φ_{H1} and φ_{H2} to describe the hydrogen molecule in minimal basis which is the minimum number of spatial functions required to describe the system. The molecular spatial orbitals are defined by symmetry: $\varphi_g = \varphi_{H1} + \varphi_{H2}$ and $\varphi_u = \varphi_{H1} - \varphi_{H2}$; which correspond to four spin-orbitals: $|\chi_1\rangle = |\varphi_g\rangle|\alpha\rangle$, $|\chi_2\rangle = |\varphi_g\rangle|\beta\rangle$, $|\chi_3\rangle = |\varphi_u\rangle|\alpha\rangle$, and $|\chi_4\rangle = |\varphi_u\rangle|\beta\rangle$. The STO-3G basis is used to evaluate the spatial integrals of the Hamiltonian which is defined as $\mathcal{H} = H^{(1)} + H^{(2)}$, where since $h_{pqrs} = h_{pqsr}$, $H^{(1)}$ and $H^{(2)}$ are simplified as^{8,31,36}

$$H^{(1)} = h_{11}a_1^\dagger a_1 + h_{22}a_2^\dagger a_2 + h_{33}a_3^\dagger a_3 + h_{44}a_4^\dagger a_4, \quad (13)$$

and

$$\begin{aligned} H^{(2)} &= h_{1221}a_1^\dagger a_2^\dagger a_2 a_1 + h_{3443}a_3^\dagger a_4^\dagger a_4 a_3 + h_{1441}a_1^\dagger a_4^\dagger a_4 a_1 \\ &+ h_{2332}a_2^\dagger a_3^\dagger a_3 a_2 + (h_{1331} - h_{1313})a_1^\dagger a_3^\dagger a_3 a_1 \\ &+ (h_{2442} - h_{2424})a_2^\dagger a_4^\dagger a_4 a_2 + (h_{1423})(a_1^\dagger a_4^\dagger a_2 a_3 \\ &+ a_3^\dagger a_2^\dagger a_4 a_1) + (h_{1243})(a_1^\dagger a_2^\dagger a_4 a_3 + a_3^\dagger a_4^\dagger a_2 a_1). \end{aligned} \quad (14)$$

Using the findings in Ref. 31 for the spatial integral values evaluated for atomic distance 1.401 a.u. in Eqs. (13) and (14), the Hamiltonian matrix found as a matrix of order 16 (see the Appendix for the Hamiltonian matrix), so four qubits are required to implement the unitary propagator of this Hamiltonian which is found from $e^{-i\mathcal{H}t}$ (see Ref. 37).

The decomposed circuit design for the unitary propagator of the hydrogen molecule is shown in Fig. 10. The circuit in Fig. 10 does not include the approximation error coming from the Trotter–Suzuki decomposition; however, it has some small errors which can be gauged from Fig. 11(a) showing the evolution of the error through the iterations of the optimization. Therefore, the evolution of the cost is given in Fig. 11(b).

The global phase with $e^{1.5i}$ is added to the beginning of the circuit in Fig. 10 which allows the phase estimation algorithm to generate more accurate results. This global phase is estimated as $\text{phase} = e^{\text{sign}(\text{Im}(p))\text{acos}(\text{Re}(p))i}$, where $p = \text{Tr}(U_a U_{H_2})/16$ and U_a is the matrix representation of the found circuit. The circuit including the global phase is also simulated within the phase estimation algorithm (for each value the IPEA is run 20 times). The phase and energy eigenvalues computed from the simulation are given in Table I with the exact eigenvalues of the Hamiltonian matrix.

C. Simulation of the water molecule

The excited states of molecular systems are difficult to resolve by employing the Hartree–Fock wave function as an initial trial state. The main reason for this difficulty is due to the fact that contributions from several configuration state functions (CSF) must be considered if one is seeking a reasonable overlap of the trial state with the exact wave function. Wang *et al.*⁶ developed a quantum algorithm to obtain

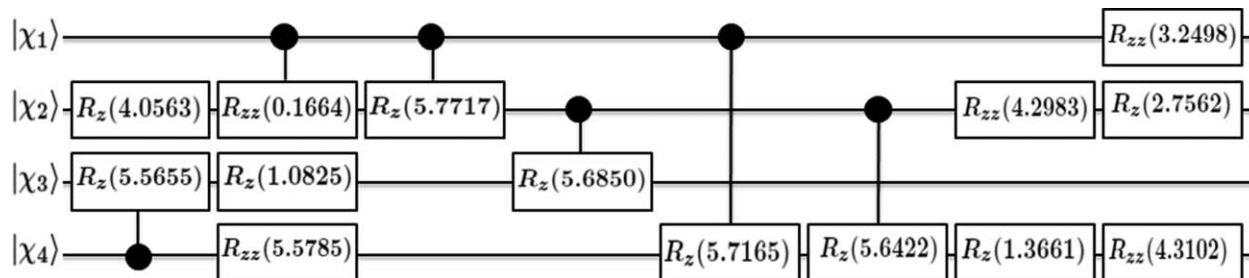


FIG. 10. The circuit design for the unitary propagator of the Hamiltonian of hydrogen molecule. The unitary propagator is found by using the spatial integral values in Ref. 31 and the definitions for the annihilation and creation operators in Eq. (8) into Eq. (13) and Eq. (14).

the energy spectrum of molecular systems based on the multi-configurational self-consistent field (MCSCF) wave function. By using a MCSCF wave function as the initial guess, the excited states are accessible. They demonstrate that such an algorithm can be used to obtain the energy spectrum of the water molecule. The geometry used in the calculation is near the equilibrium geometry (OH distance $R = 1.8435 a_0$ and the angle HOH = 110.57). With a complete active space type

MCSCF method for the excited-state simulation, the CI space is composed of 18 CSFs, so five-qubits are required to represent the wave function.

After finding the molecular Hamiltonian \mathcal{H} as a matrix of order 18, we deploy the same idea as in Ref. 38 and define the unitary operator as

$$\hat{U}_{H_2O} = e^{i\tau(E_{\max} - \mathcal{H})t} \quad (15)$$

where τ is defined as

$$\tau = \frac{2\pi}{E_{\max} - E_{\min}}. \quad (16)$$

E_{\max} and E_{\min} are the expected maximum and minimum energies. The choice of E_{\max} and E_{\min} must cover all the eigenvalues of the Hamiltonian to obtain the correct results. The final energy E_j is found from the expression

$$E_j = E_{\max} - \frac{2\pi\phi_j}{\tau}, \quad (17)$$

where ϕ_j is the corresponding phase of the E_j . Since the eigenvalues of the Hamiltonian of the water molecule are between $-80 \pm \epsilon$ and $-84 \pm \epsilon$ ($\epsilon \leq 0.1$) taking $E_{\max} = 0$ and $E_{\min} = -200$ gives the following:

$$\hat{U} = e^{\frac{-i2\pi H}{200}t}. \quad (18)$$

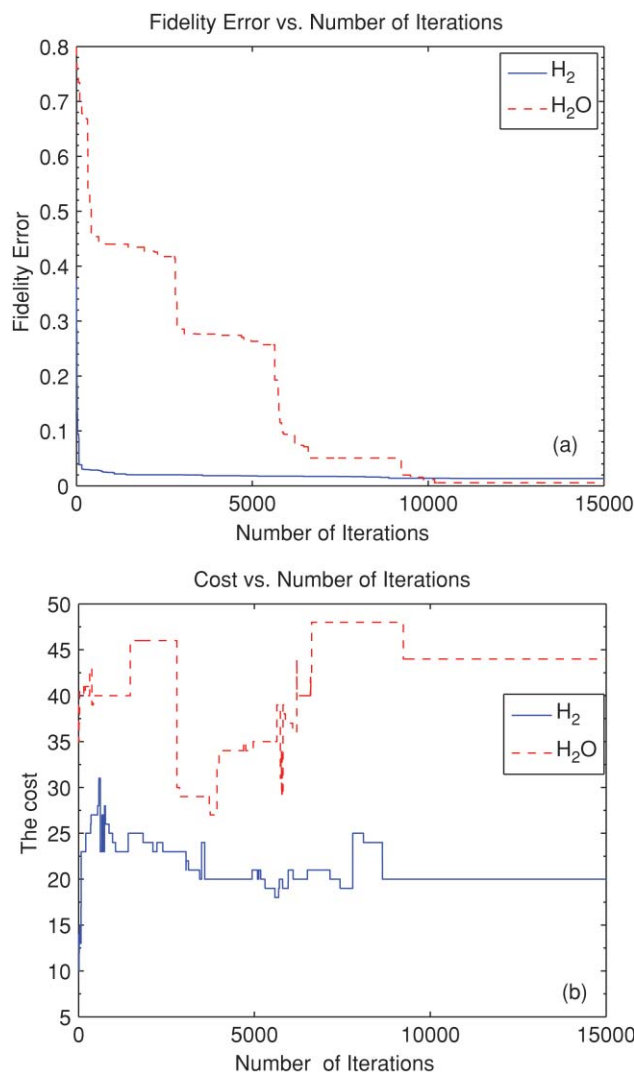


FIG. 11. The evolutions of the cost and the error in the optimization for the exponentials of the Hamiltonians of the water and the hydrogen molecules.

TABLE I. The found and the corresponding exact eigenvalues of the Hamiltonian of the hydrogen molecule.

Phase	Found energies	Exact energies
0.0139	-0.0872	0.0000
0.0314	-0.1971	0.2064
0.0404	-0.2536	-0.2339
0.0433	-0.2720	-0.3613
0.0685	-0.4304	-0.3613
0.0982	-0.6171	-0.4759
0.1204	-0.7564	-0.4759
0.1676	-1.0531	-0.8836
0.1753	-1.1015	-1.1607
0.1765	-1.1089	-1.1607
0.1862	-1.1698	-1.2462
0.2127	-1.3362	-1.2462
0.2136	-1.3422	-1.2462
0.2257	-1.4179	-1.2525
0.2313	-1.4534	-1.2525
0.2894	-1.8182	-1.8511

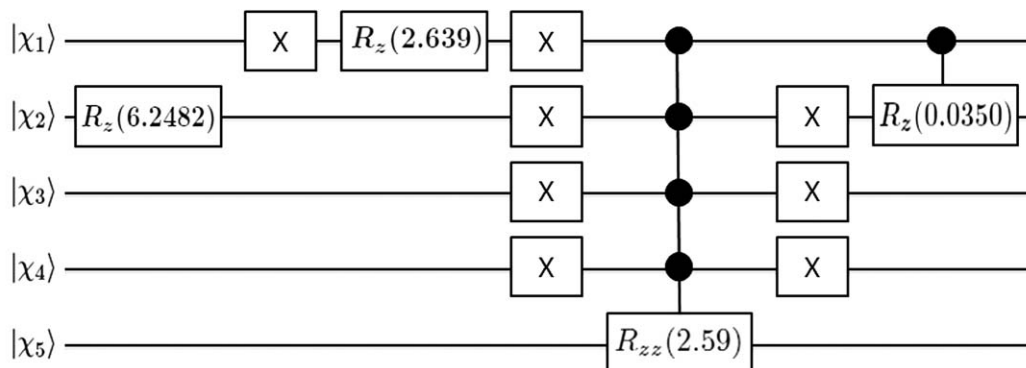


FIG. 12. The circuit design for the unitary propagator of the water molecule.

Figure 12 shows the circuit diagram for this unitary operator. The cost of the circuit is 44 [see Fig. 11(b)] determined by summing up the cost of each gates in the circuit. The evolution of the fidelity error with respect to the number of iterations is plotted in Fig. 11(a). Since we take E_{\max} as zero, this deployment does not require any extra quantum gate for the implementation within the phase estimation algorithm. The simulation of this circuit within the iterative PEA results the phase and energy eigenvalues given in Table II: the left two columns are the computed phases and the corresponding energies, respectively, while the rightmost column of the matrix is the eigenvalues of the Hamiltonian of the water molecule (for each value of the phase, the IPEA is run 20 times).

V. CONCLUSION

To be able to simulate Hamiltonians of atomic and molecular systems and also apply quantum algorithms to solve different kinds of problems on quantum computers, it

TABLE II. The found and the exact energy eigenvalues of the water molecule.

Phase	Found energy	Exact energy
0.4200	-84.0019	-84.0021
0.4200	-84.0019	-83.4492
0.4200	-84.0019	-83.0273
0.4200	-84.0019	-82.9374
0.4200	-84.0019	-82.7719
0.4200	-84.0019	-82.6496
0.4200	-84.0019	-82.5252
0.4200	-84.0019	-82.4467
0.4144	-82.8884	-82.3966
0.4144	-82.8884	-82.2957
0.4144	-82.8884	-82.0644
0.4144	-82.8884	-81.9872
0.4144	-82.8884	-81.8593
0.4144	-82.8884	-81.6527
0.4144	-82.8884	-81.4592
0.4144	-82.8884	-81.0119
0.4122	-82.4423	-80.9065
0.4122	-82.4423	-80.6703

is necessary to find implementable quantum circuit designs including the minimum cost and number of quantum gate sequences. Since deterministic-efficient quantum circuit design methodology is an open problem, we applied stochastic evolutionary optimization algorithm, GLOA, to search a quantum circuit design for the given unitary matrix representing a quantum algorithm or the unitary propagator of a molecular Hamiltonian. In this paper, in addition to explaining the ways of the implementation and design of the optimization problem, we give circuit designs for the Grover search algorithm, the Toffoli gate, the quantum Fourier transform, and the quantum teleportation. Moreover, we find the circuit designs for the simulations of the water molecule and the hydrogen molecule by decomposing the unitary matrix operators found by following the fermionic model of quantum computation and then simulate them within the phase estimation algorithm. In the case of the hydrogen molecule we found that the number of gates needed to simulate the unitary operator is 14 quantum gates (excluding the global phase) with the cost of 20. For the water molecule the cost of the number of operations is found to be 44 from the definition of the cost. The approach is general and can be applied to generate the sequence of quantum gates for larger molecular systems. Research is underway to generate the quantum circuit design for the simulation of the molecular Hamiltonian of CH_2 .³⁸

ACKNOWLEDGMENTS

We would like to thank the NSF Center for Quantum Information and Computation for Chemistry, award number CHE-1037992, for financial support of this project.

APPENDIX

The matrix representation of quantum gates and algorithms used in the optimization as follows:^{1,20,27}

X , Y , and Z gates which are the Pauli operators σ_x , σ_y , and σ_z and Hadamard gate:

$$\begin{aligned}
 X &= \begin{pmatrix} 0 & 1 \\ 1 & 0 \end{pmatrix}, & Y &= \begin{pmatrix} 0 & -i \\ i & 0 \end{pmatrix}, \\
 Z &= \begin{pmatrix} 1 & 0 \\ 0 & -1 \end{pmatrix}, & H &= \frac{1}{\sqrt{2}} \begin{pmatrix} 1 & 1 \\ 1 & -1 \end{pmatrix}.
 \end{aligned}
 \tag{A1}$$

S gate and T, $\frac{\pi}{8}$, gate are

$$S = \begin{pmatrix} 1 & 0 \\ 0 & i \end{pmatrix}, T = \begin{pmatrix} 1 & 0 \\ 0 & \exp\left(i\frac{\pi}{4}\right) \end{pmatrix}. \quad (\text{A2})$$

Square root of NOT (X) gate and its complex conjugate are

$$V = \frac{1}{2} \begin{pmatrix} 1+i & 1-i \\ 1-i & 1+i \end{pmatrix}, V^\dagger = \frac{1}{2} \begin{pmatrix} 1-i & 1+i \\ 1+i & 1-i \end{pmatrix}. \quad (\text{A3})$$

Rotation gates are

$$R_x(\theta) = \begin{pmatrix} \cos\left(\frac{\theta}{2}\right) & i \sin\left(\frac{\theta}{2}\right) \\ i \sin\left(\frac{\theta}{2}\right) & \cos\left(\frac{\theta}{2}\right) \end{pmatrix},$$

$$R_y(\theta) = \begin{pmatrix} \cos\left(\frac{\theta}{2}\right) & \sin\left(\frac{\theta}{2}\right) \\ -\sin\left(\frac{\theta}{2}\right) & \cos\left(\frac{\theta}{2}\right) \end{pmatrix}, \quad (\text{A4})$$

$$R_z(\theta) = \begin{pmatrix} 1 & 0 \\ 0 & \exp(i\theta) \end{pmatrix},$$

$$R_{zz}(\theta) = \begin{pmatrix} \exp(i\theta) & 0 \\ 0 & \exp(i\theta) \end{pmatrix}.$$

The matrix representation of the Toffoli gate is as follows:

$$\begin{pmatrix} 1 & 0 & 0 & 0 & 0 & 0 & 0 & 0 \\ 0 & 1 & 0 & 0 & 0 & 0 & 0 & 0 \\ 0 & 0 & 1 & 0 & 0 & 0 & 0 & 0 \\ 0 & 0 & 0 & 1 & 0 & 0 & 0 & 0 \\ 0 & 0 & 0 & 0 & 1 & 0 & 0 & 0 \\ 0 & 0 & 0 & 0 & 0 & 1 & 0 & 0 \\ 0 & 0 & 0 & 0 & 0 & 0 & 0 & 1 \\ 0 & 0 & 0 & 0 & 0 & 0 & 1 & 0 \end{pmatrix}. \quad (\text{A5})$$

The matrix representation of the sender part of the quantum teleportation is as follows:^{10,40}

$$\frac{1}{2} \begin{pmatrix} 1 & 0 & -1 & 0 & 0 & 1 & 0 & 1 \\ 0 & 1 & 0 & -1 & 1 & 0 & 1 & 0 \\ 0 & 1 & 0 & 1 & 1 & 0 & -1 & 0 \\ 1 & 0 & -1 & 0 & 0 & 1 & 0 & 1 \\ -1 & 0 & -1 & 0 & 0 & 1 & 0 & 1 \\ 0 & -1 & 0 & 1 & 1 & 0 & 1 & 0 \\ 0 & -1 & 0 & -1 & 1 & 0 & -1 & 0 \\ -1 & 0 & -1 & 0 & 0 & 1 & 0 & -1 \end{pmatrix}.$$

The Hamiltonian of the hydrogen molecule which is found by using the spatial integral values in Ref. 31 is as follows:

$$\begin{pmatrix} 0.2064 & 0 & 0 & 0 & 0 & 0 & 0 & 0 & 0 & 0 & 0 & 0 & 0 & 0 & 0 \\ 0 & -1.1607 & 0 & 0 & 0 & 0 & 0 & 0 & 0 & 0 & 0 & 0 & 0 & 0 & 0 \\ 0 & 0 & -1.1607 & 0 & 0 & 0 & 0 & 0 & 0 & 0 & 0 & 0 & 0 & 0 & 0 \\ 0 & 0 & 0 & -1.8305 & 0 & 0 & 0 & 0 & 0 & 0 & 0.1813 & 0 & 0 & 0 & 0 \\ 0 & 0 & 0 & 0 & -0.3613 & 0 & 0 & 0 & 0 & 0 & 0 & 0 & 0 & 0 & 0 \\ 0 & 0 & 0 & 0 & 0 & -1.2462 & 0 & 0 & 0 & 0 & 0 & 0 & 0 & 0 & 0 \\ 0 & 0 & 0 & 0 & 0 & 0 & -1.0649 & 0 & -0.1813 & 0 & 0 & 0 & 0 & 0 & 0 \\ 0 & 0 & 0 & 0 & 0 & 0 & 0 & -1.2525 & 0 & 0 & 0 & 0 & 0 & 0 & 0 \\ 0 & 0 & 0 & 0 & 0 & 0 & 0 & 0 & -0.3613 & 0 & 0 & 0 & 0 & 0 & 0 \\ 0 & 0 & 0 & 0 & 0 & 0 & -0.1813 & 0 & 0 & -1.0649 & 0 & 0 & 0 & 0 & 0 \\ 0 & 0 & 0 & 0 & 0 & 0 & 0 & 0 & 0 & -1.2462 & 0 & 0 & 0 & 0 & 0 \\ 0 & 0 & 0 & 0 & 0 & 0 & 0 & 0 & 0 & 0 & -1.2525 & 0 & 0 & 0 & 0 \\ 0 & 0 & 0 & 0.1813 & 0 & 0 & 0 & 0 & 0 & 0 & 0 & -0.2545 & 0 & 0 & 0 \\ 0 & 0 & 0 & 0 & 0 & 0 & 0 & 0 & 0 & 0 & 0 & 0 & -0.4759 & 0 & 0 \\ 0 & 0 & 0 & 0 & 0 & 0 & 0 & 0 & 0 & 0 & 0 & 0 & 0 & -0.4759 & 0 \\ 0 & 0 & 0 & 0 & 0 & 0 & 0 & 0 & 0 & 0 & 0 & 0 & 0 & 0 & 0 \end{pmatrix}$$

¹M. A. Nielsen and I. L. Chuang, *Quantum Computation and Quantum Information* (Cambridge University Press, New York, USA, 2000).

²D. A. Lidar, I. L. Chuang, and K. B. Whaley, *Phys. Rev. Lett.* **81**, 2594 (1998).

³J. R. West, D. A. Lidar, B. H. Fong, M. F. Gyure, X. Peng, and D. Suter (2009), arXiv:0911.2398v1.

⁴D. S. Abrams and S. Lloyd, *Phys. Rev. Lett.* **83**, 5162 (1999).

⁵A. Aspuru-Guzik, A. D. Dutoi, P. J. Love, and M. Head-Gordon, *Science* **309**, 1704 (2005).

⁶H. Wang, S. Kais, A. Aspuru-Guzik, and M. R. Hoffmann, *Phys. Chem. Chem. Phys.* **10**, 5388 (2008).

⁷D. A. Lidar and H. Wang, *Phys. Rev. E* **59**, 2429 (1999).

⁸B. P. Lanyon, J. D. Whitfield, G. G. Gillett, M. E. Goggin, M. P. Almeida, I. Kassal, J. D. Biamonte, M. Mohseni, B. J. Powell, M. Barbieri, A. Aspuru-Guzik, and A. G. White, *Nat. Chem.* **2**, 106 (2010).

⁹C. P. Williams and A. G. Gray, in *Quantum Computing and Quantum Communications* (Springer, Berlin / Heidelberg, 1999) pp. 113–125.

¹⁰T. Yabuki and H. Iba, in *In Late Breaking Papers at the 2000 Genetic and Evolutionary Computation Conference* (Morgan Kaufman Publishers, San Francisco, California, 2000) pp. 421–425.

¹¹F. Peng, G. jun Xie, and T. hao Wu, Automatic Synthesis of Quantum Teleportation Circuit *Proceedings of the 2009 Fourth International*

- Conference on Computer Sciences and Convergence Information Technology ICCIT '09* (IEEE Computer Society, Washington, DC, USA, 2009) pp. 70–74.
- ¹²L. Spector, *Automatic Quantum Computer Programming: A Genetic Programming Approach (Genetic Programming)* (Springer-Verlag, New York, 2006).
- ¹³R. Stadelhofer, W. Banzhaf, and D. Suter, *AI EDAM* **22**, 285 (2008).
- ¹⁴A. Leier, Evolution of Quantum Algorithms using Genetic Programming, Ph.D. thesis, Dortmund University, Germany (2004).
- ¹⁵M. Lukac and M. Perkowski, in *EH '02: Proceedings of the 2002 NASA/DoD Conference on Evolvable Hardware (EH'02)* (IEEE Computer Society, Washington, 2002), p. 177.
- ¹⁶P. Massey, J. A. Clark, and S. Stepney, in *GECCO (2)* (2004), pp. 569–580.
- ¹⁷A. Gepp and P. Stocks, *Genetic Programming and Evolvable Machines* **10**, 181 (2009).
- ¹⁸A. Daskin and S. Kais, *Mol. Phys.* **109**, 761 (2011).
- ¹⁹G. Vidal, *Phys. Rev. Lett.* **93**, 040502 (2004).
- ²⁰A. Barenco, C. H. Bennett, R. Cleve, D. P. DiVincenzo, N. Margolus, P. Shor, T. Sleator, J. A. Smolin, and H. Weinfurter, *Phys. Rev. A* **52**, 3457 (1995).
- ²¹J. F. Miller and S. L. Harding, in *GECCO '08: Proceedings of the 2008 GECCO conference companion on Genetic and evolutionary computation* (ACM, New York, 2008), pp. 2701–2726.
- ²²P. Serra, A. F. Stanton, and S. Kais, *Phys. Rev. E* **55**, 1162 (1997).
- ²³P. Nigra and S. Kais, *Chem. Phys. Lett.* **305**, 433 (1999).
- ²⁴P. Serra, A. F. Stanton, S. Kais, and R. E. Bleil, *J. Chem. Phys.* **106**, 7170 (1997).
- ²⁵D. P. DiVincenzo, *Proc. R. Soc. London* **454**, 261 (1998).
- ²⁶L. K. Grover, in *Proceedings of the twenty-eighth annual ACM symposium on Theory of computing* (ACM, New York, 1996), pp. 212–219.
- ²⁷P. Kaye, R. Laflamme, and M. Mosca, *An Introduction to Quantum Computing* (Oxford University Press, New York, 2007).
- ²⁸G. Brassard, S. L. Braunstein, and R. Cleve, *Physica D* **120**, 43 (1998).
- ²⁹G. Ortiz, J. E. Gubernatis, E. Knill, and R. Laflamme, *Phys. Rev. A* **64**, 022319 (2001).
- ³⁰C. D. Batista and G. Ortiz, *Phys. Rev. Lett.* **86**, 1082 (2001).
- ³¹J. D. Whitfield, J. Biamonte, and A. Aspuru-Guzik, *Mol. Phys.* **109**, 735 (2011).
- ³²E. Ovrum and M. Hjorth-Jensen, *Quantum computation algorithm for many-body studies*, Tech. Rep. arXiv:0705.1928 (2007).
- ³³M. Dobšiček, G. Johansson, V. Shumeiko, and G. Wendin, *Phys. Rev. A* **76**, 030306 (2007).
- ³⁴A. Kitaev, *Quantum Measurements and the Abelian Stabilizer Problem*, (1995) arXiv:quant-ph/9511026.
- ³⁵C. P. Williams, in *Explorations in Quantum Computing* (Springer, London, 2011), pp. 349–367.
- ³⁶I. Kassal, J. D. Whitfield, A. Perdomo-Ortiz, M.-H. Yung, and A. Aspuru-Guzik, *Ann. Rev. Phys. Chem.* **62**, 185 (2011).
- ³⁷The time t in the equation is taken as 1. For the matrix exponentiation, we used the matlab function *expm* which uses the Pade approximation with scaling and squaring. See also Ref. 39.
- ³⁸L. Veis and J. Pittner, *J. Chem. Phys.* **133**, 194106 (2010).
- ³⁹N. J. Higham, *SIAM J. Matrix Anal. Appl.* **26**, 2005 (2005).
- ⁴⁰T. Reid, *On the evolutionary design of quantum circuits*, Master's thesis, Waterloo University, Ontario, Canada (2005).